DESIGN MODELS FOR SHEAR STRENGTHENING OF REINFORCED CONCRETE BEAMS WITH EXTERNALLY BONDED FRP COMPOSITES: A STATISTICAL VS RELIABILITY APPROACH

J.L.T. LIMA [1]   J.A.O BARROS [2]

[1] MSc Student;   [2] Associate Prof., Department of Civil Engineering, University of Minho, Portugal

Keywords: analytical, bonded, externally, FRP, models, shear, strengthening

1   INTRODUCTION

Experimental studies conducted worldwide on reinforced concrete (RC) beams strengthened in shear with externally bonded (EBR) fiber-reinforced polymers (FRP) over the last years evince the reliability and efficacy of such technique for structural retrofitting. For elements with shear resistance deficiencies, an higher load carrying capacity may be achieved by bonding FRP reinforcement systems with the fibers as orthogonal as practically possible to the critical shear crack plane for an optimal configuration, or with the fibers normal to the beam axis for a more practical setting. Common configurations of strengthening (Fig.1) include the full wrapping of the cross section (O), U jacketing along 3 sides (U) and side bonding in the beam web (S). Additional mechanical anchorage systems can be provided to enhance the behavior of U or S configurations where the available bond length is short (U+ and S+).
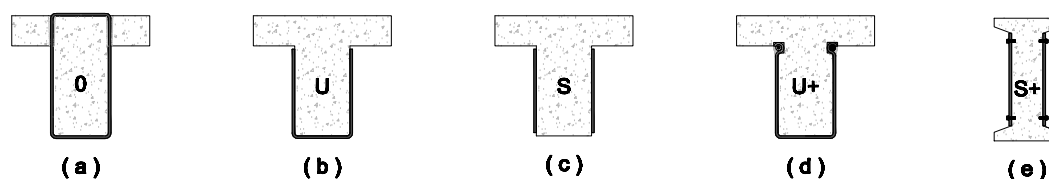

Fig. 1: Common externally bonded FRP strengthening configurations

Each of the aforementioned strengthening configurations may be set in several possible arrangements (Fig. 2) regarding the fiber orientation, the use of discrete strips or continuous sheets, and the overlay of sheets with different fiber orientations, among others.
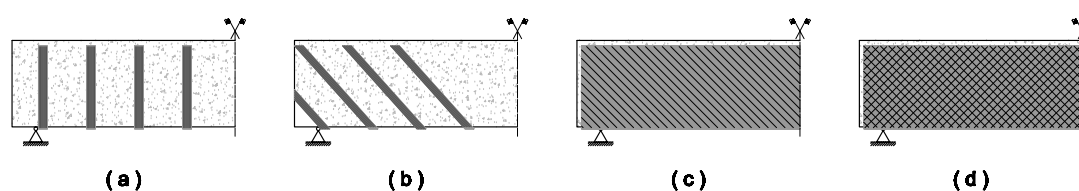

Fig. 2: Possible arrangements for externally bonded FRP strengthening

2   ANALYTICAL FORMULATIONS FOR FRP SHEAR REINFORCEMENT DESIGN

As an outcome of the increasing demand stimulated by a continuous growth in field applications, several proposed analytical formulations [1-3] have been implemented into reference design guidelines, providing the guidance for design, detailing, and installation of FRP based strengthening systems. The present study addresses the shear provisions included in *fib* [4], ACI [5], CNR [6] and the Australian Standard [7] design guidelines. The later follows an analytical model previously introduced by Chen and Teng (CT) [8, 9]. All of the aforementioned design models rely on the approach where shear strength of a strengthened member is attained by the sum of the contributions from the reinforcing steel, V_s, and concrete, V_c, with the one deriving from the FRP ,V_f, as follows:

$$V_r = V_c + V_s + V_f \tag{1}$$

where V_c and V_s, may be calculated according to provisions existing on current design codes, independently of the FRP strengthening system adopted. The methodology to estimate the design value of the FRP contribution in shear, V_{fd}, according to each of the aforementioned design proposals is briefly described in Table 1. Figure 1 summarizes the adopted notation defining the geometric properties of a generic beam reinforced in shear with externally bonded FRP.
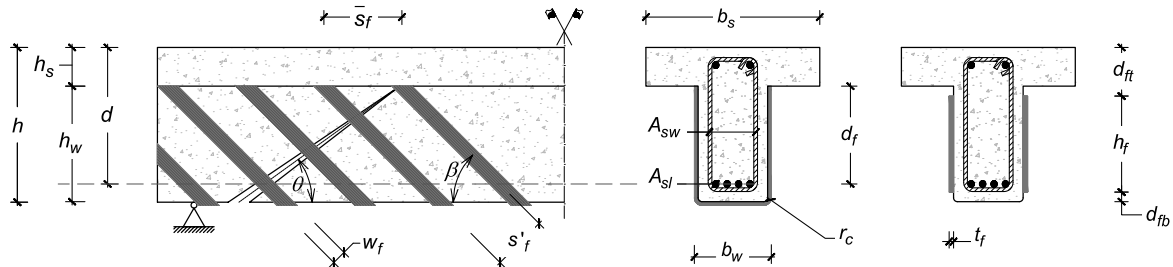

Fig. 3: Adopted notation to define the main geometric properties of an FRP shear reinforcement

Table 1: V_{fd} calculation methodology (cont.)

fib design proposal:	ACI design proposal:
$$V_{fd} = 0.9 \cdot \varepsilon_{fed} \cdot E_f \cdot \rho_f \cdot b_w \cdot d \cdot (\cot\theta + \cot\beta) \cdot \sin\beta$$ $$\rho_f = \frac{2 \cdot t_f \cdot w_f}{b_w \cdot \overline{s_f}} \text{ (strips) } ; \quad \rho_f = \frac{2 \cdot t_f \cdot \sin\beta}{b_w} \text{ (cont.)}$$ $$\varepsilon_{fed} = \frac{0.8 \cdot \varepsilon_{fe}}{\gamma_f} \quad ; \quad \gamma_f = 1.2 \; / \; 1.3 \; / \; 1.35$$ *i)* Full wrapping configuration (O): $$\varepsilon_{fe} = 0.17 \cdot \left(\frac{f_{cm}^{\frac{2}{3}}}{E_f \cdot \rho_f / 1000} \right)^{0.30} \cdot \varepsilon_{fu}$$ *ii)* Side bonding or U jacketing configuration (U, S): $$\varepsilon_{fe} = \min \begin{cases} 0.65 \cdot \left(\dfrac{f_{cm}^{\frac{2}{3}}}{E_f \cdot \rho_f / 1000} \right)^{0.56} \cdot 10^{-3} \\[2ex] 0.17 \cdot \left(\dfrac{f_{cm}^{\frac{2}{3}}}{E_f \cdot \rho_f / 1000} \right)^{0.30} \cdot \varepsilon_{fu} \end{cases}$$	$$V_{fd} = \phi \cdot \psi_f \cdot \left(2 \cdot t_f \cdot \frac{w_f}{\overline{s_f}} \cdot f_{fe} \cdot (\sin\beta + \cos\beta) \cdot d_f \right)$$ $$\phi = 0.85 \; ; \; \psi_f = 0.95 \text{ (O)} \; ; \; \psi_f = 0.85 \text{ (U,S)}$$ $$f_{fe} = E_f \cdot \varepsilon_{fe}$$ *i)* Full wrapping configuration (O): $$\varepsilon_{fe} = 0.004 \le 0.75 \cdot \varepsilon_{fu}$$ *ii)* Side bonding or U jacketing configuration (U, S): $$\varepsilon_{fe} = k_v \cdot \varepsilon_{fu} \le 0.004$$ $$k_v = \frac{k_1 \cdot k_2 \cdot L_e}{11900 \cdot \varepsilon_{fu}} \le 0.75$$ $$k_1 = \left(\frac{f_{ck}}{27} \right)^{2/3} \quad ; \quad L_e = \frac{23300}{(t_f \cdot E_f)^{0.58}}$$ $$k_2 = \frac{d_f - L_e}{d_f} \text{ (U) } ; \; k_2 = \frac{d_f - 2 \cdot L_e}{d_f} \text{ (S)}$$

Notation:

ε_{fed} - design value of effective FRP strain;	ϕ - shear strength reduction factor [10];
ε_{fe} - mean value of effective FRP strain;	ψ_f - additional reduction factor for FRP;
ε_{fu} - FRP ultimate tensile strain;	k_v - bond reduction coefficient;
γ_f - partial factor for FRP reinforcement;	k_1 - modif. factor regarding the concrete strength;
ρ_f - FRP reinforcement ratio;	k_2 - modif. factor regarding the FRP configuration;
E_f - elasticity modulus of FRP reinforcement;	L_e - effective bond length of FRP reinforcement;
f_{cm} - concrete average compressive strength;	f_{ck} - concrete characteristic compressive strength;

Table 1 (cont.): V_{fd} calculation methodology

CNR design proposal:

i) Full Wrapping configuration (O)

$$V_{fd} = \frac{1}{\gamma_{Rd}} \cdot 0.9 \cdot d \cdot f_{fed} \cdot 2 \cdot t_f \cdot (\cot\theta + \cot\beta) \cdot \frac{w_f}{s_f'}$$

$$f_{fed} = f_{fdd} \cdot \left[1 - \frac{1}{6} \cdot \frac{L_e \cdot \sin\beta}{\min\{0.9 \cdot d, h_w\}} \right] +$$

$$+ \underbrace{\frac{1}{2}(\phi_R \cdot f_{fd} - f_{fdd}) \cdot \left[1 - \frac{L_e \cdot \sin\beta}{\min\{0.9 \cdot d, h_w\}} \right]}_{\geq 0}$$

$$\phi_R = 0.2 + 1.6 \cdot \frac{r_c}{b_w} \quad ; \quad 0 \leq \frac{r_c}{b_w} \leq 0.5$$

$$L_e = \sqrt{\frac{E_f \cdot t_f}{2 \cdot f_{ctm}}} \quad ; \quad f_{fdd} = \frac{0.80}{\gamma_{fd}} \cdot \sqrt{\frac{2 \cdot E_f \cdot G_{fk}}{t_f}}$$

$$G_{fk} = 0.03 \cdot k_b \cdot \sqrt{f_{ck} \cdot f_{ctm}} \quad ; \quad k_b = \sqrt{\frac{2 - w_f/s_f'}{1 + b_f/400}} \geq 1$$

ii) U jacket configuration (U)

$$f_{fed} = f_{fdd} \cdot \left[1 - \frac{1}{3} \cdot \frac{L_e \cdot \sin\beta}{\min\{0.9 \cdot d, h_w\}} \right]$$

iii) Side bonding configuration (S)

$$V_{fd} = \frac{1}{\gamma_{Rd}} \cdot \min\{0.9 \cdot d, h_w\} \cdot f_{fed} \cdot 2 \cdot t_f \cdot \frac{\sin\beta}{\sin\theta} \cdot \frac{w_f}{s_f'}$$

$$f_{fed} = f_{fdd} \cdot \frac{z_{red,eq}}{\min\{0.9 \cdot d, h_w\}} \cdot \left(1 - 0.6 \cdot \sqrt{\frac{L_{eq}}{z_{red,eq}}} \right)^2$$

$$z_{red,eq} = z_{red} + L_{eq}$$

$$z_{red} = \min\{0.9 \cdot d, h_w\} - L_e \cdot \sin\beta$$

$$L_{eq} = \frac{s_{uf}}{f_{fdd}/E_f} \cdot \sin\beta$$

CIDAR (CT) design proposal:

$$V_{fd} = 2 \cdot f_{fed} \cdot t_f \cdot \frac{w_f}{s_f'} \cdot h_{fe} \cdot (\cot\theta + \cot\beta) \cdot \sin\beta$$

$$h_{fe} = z_b - z_t \quad ; \quad z_b = 0.9 \cdot d - d_{fb} \quad ; \quad z_t = d_{ft}$$

$$f_{fed} = D_f \cdot f_{fd,max}$$

i) Failure by FRP rupture (O)

$$D_f = 0.5 \cdot \left(1 + \frac{z_t}{z_b} \right)$$

$$f_{fd,max} = \begin{cases} \dfrac{1}{\gamma_f} \cdot \phi_R \cdot f_{fu}, & \varepsilon_f \leq 1.5\% \\[2mm] \dfrac{1}{\gamma_f} \cdot \phi_R \cdot E_f \cdot \varepsilon_f, & \varepsilon_f > 1.5\% \end{cases}$$

$$\phi_R = 0.80 \; ; \; \gamma_f = 1.25$$

ii) Failure by FRP debonding (U , S)

$$D_f = \begin{cases} \dfrac{2}{\pi \cdot \lambda} \cdot \dfrac{1 - \cos\left(\frac{\pi}{2} \cdot \lambda\right)}{\sin\left(\frac{\pi}{2} \cdot \lambda\right)}, & \lambda \leq 1 \\[2mm] 1 - \dfrac{\pi - 2}{\pi \cdot \lambda}, & \lambda > 1 \end{cases} \quad ; \quad \lambda = L_{max}/L_e$$

$$L_{max} = \begin{cases} \dfrac{h_{fe}}{\sin\beta}, & \text{(U)} \\[2mm] \dfrac{h_{fe}}{2 \cdot \sin\beta}, & \text{(S)} \end{cases} \quad ; \quad L_e = \sqrt{\frac{E_f \cdot t_f}{\sqrt{f_{ck}}}}$$

$$f_{fd,max} = \min \begin{cases} \dfrac{1}{\gamma_f} \cdot \phi_R \cdot f_{fu} \\[2mm] \dfrac{1}{\gamma_f} \cdot 0.35 \cdot \beta_L \cdot \beta_w \cdot \sqrt{\dfrac{E_f \cdot \sqrt{f_{ck}}}{t_f}} \end{cases}$$

$$\beta_L = \begin{cases} \lambda, & \lambda \leq 1 \\ 1, & \lambda > 1 \end{cases} \quad ; \quad \beta_w = \sqrt{\frac{2 - w_f/(s_f \cdot \sin\beta)}{1 + w_f/s_f \cdot \sin\beta}}$$

Notation:

γ_{Rd} - partial factor for the resistance model (1.2);
f_{ctm} - average concrete tensile strength;
f_{fed} - design value for the FRP effective stress;
f_{fd} - design value for the ultimate FRP stress;
f_{fdd} - design value for the FRP debonding stress;
G_{fk} - bonded joint specific fracture energy;
k_b - covering / scale coefficient;
s_{uf} - FRP slip at debonding (0.20mm);

ϕ_R - reduction factor due to local stress in corners;
λ - normalized maximum bond length;
D_f - stress distribution factor;
$f_{fd,max}$ - maximum design stress in FRP;
f_{fu} - ultimate FRP tensile stress;
h_{fe} - effective height of the bonded reinforcement;
β_L - bond length coefficient;
β_w - strip width coefficient;

3   PERFORMANCE APPRAISAL OF THE ANALYTICAL FORMULATIONS

3.1   Database assembly

To assess the accuracy of the theoretical predictions obtained with the aforementioned analytical formulations, a database (DB) containing the experimental results from 212 beams strengthened with EBR was collected from published literature, upgrading previous compiled databases [11-12]. The criteria adopted in this task was to collect the largest amount of data with a wide spectrum of test results regarding the beams geometry, concrete properties, longitudinal steel reinforcement ratios, shear steel reinforcement ratios, FRP properties and strengthening configurations. Aiming to reduce the influence of erroneous and inconsistent data present in the DB, the analysis was performed not only in the integral database (IDB), but also in partial subsets of the data – reduced databases (RDB). Detailed information on the databases characteristics and the considered beams may be found in [13].

3.2   Results obtained using the integral database (IDB)

For each described design model, the obtained values of V_{fd} are compared with $V_{f,exp}$ and a χ factor corresponding to the $V_{f,exp}/V_{fd}$ ratio is evaluated. Figure 4 plots the predicted against experimental values, where a 45° solid line establishes the division between the safe previsions from the unconservative ones and a dashed line traces an "ideal safety trend" corresponding to χ=1.5.
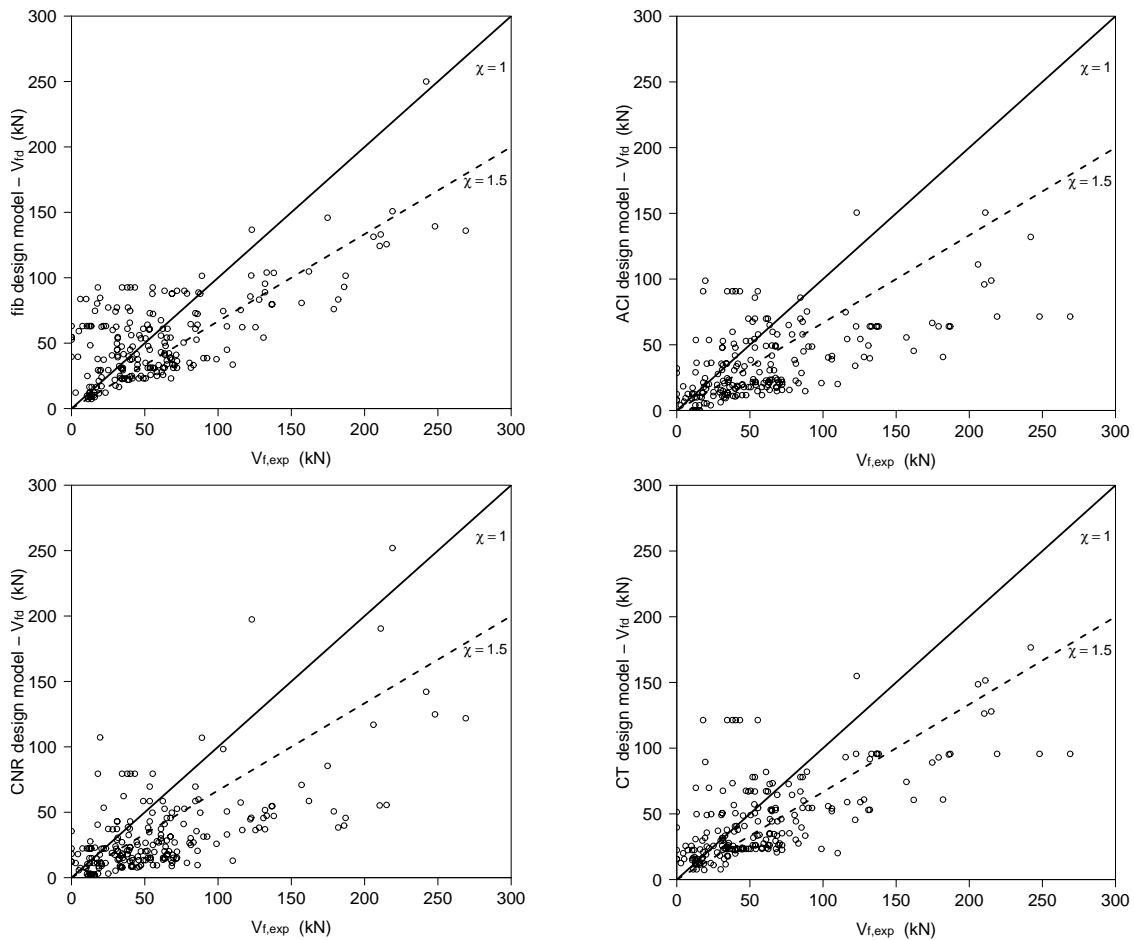

Fig. 4 - $V_{f,exp}$ *vs* V_{fd} scatterplots regarding *fib*, ACI, CNR and CT design models

A large scatter is observed in the experimental *vs* predicted design values for all of the considered analytical formulations. Table 2 summarizes the main descriptive statistical measures regarding the χ factor, namely minimum (MIN) and maximum (MAX) values, the average (AVG) that represents a global safety factor associated with the design procedure, the standard deviation (STD) and the coefficient of variation (COV) that are indicators of accuracy. The first quartile (Q1) that cuts off the lowest 25% of data, the median (MED) corresponding to the 50th percentile and the third quartile (Q3) that cuts off the highest 25% of data are also included.

4

Table 2: Statistical values of the χ factor computed from the IDB

χ	Min	Q1	MED	AVG	Q3	MAX	STD	COV
FIB	0.00	0.730	1.198	1.22	1.718	3.278	0.666	0.546
ACI	0.00	0.980	1.903	2.017	2.831	5.961	1.255	0.622
CNR	0.00	1.126	2.108	2.528	3.541	9.261	1.846	0.730
CT	0.00	0.875	1.370	1.431	1.962	5.454	0.826	0.577

The obtained results show that the *fib* design model presents, in average, the lowest safety factor while the safest predictions are attained with CNR. The largest scattering is attained by the CNR model (COV=0.73) while the least scattered model is fib (COV=0.55). The CT model globally presents a good performance with an average value of χ =1.43 and COV = 0.58.

However, from the structural safety point of view, a classification system based only on the main descriptive statistics measures regarding the behavior of the χ factor may not provide enough information to assess the reliability of a design proposal, considering that for structural purposes having χ=0.5 is worst than χ=2.0, which is not taken into account on the statistical analysis.

To overcome this limitation a weighed penalty classification system was applied, based on the "Demerit Points Classification" (DPC) model proposed by [14], where a penalty (PEN) is assigned to each range of χ ratios according to Table 3, and the total of penalties determines the performance of each design model.

Table 3: Reliability analysis based on structural safety – IBD

χ	Classification	PEN	FIB	ACI	CNR	CT
< 0.75	Extr. Dangerous	10	55	32	28	45
0.75 - 1.00	Dangerous	5	30	22	15	23
1.00 - 1.25	Reduced Safety	2	26	18	16	30
1.25 - 1.75	Appropriate Safety	0	53	26	27	43
1.75 - 3.00	Conservative	1	47	65	58	65
> 3.00	Extr. Conservative	2	1	42	68	6
		∑ PEN	801	615	581	702

From Table 3 it can be noticed that the *fib* design model presents the weakest performance, with the highest number of penalty points corresponding to 40% of Predictions Against Safety (PAS, χ<1), while the best results are attained by the CNR design proposal with the lowest of number of PAS (20%). The CNR model also provides the highest number of extremely conservative values (32%).

3.3   Results obtained using the RDB

The high scattering found in the previous analysis performed over a DB with 212 beams with highly differentiated characteristics, proves that none of the studied design models simulates with enough accuracy the generic behavior of RC beams strengthened in shear with externally bonded CFRP. It was also found that all the aforementioned design proposals provided a large amount of unsafe values for V_{fd}, especially in the range $0 < V_{f,exp} < 100$ kN. Such can be related with a significant number of experimental results where, without a clear understanding, the load carrying increase due to the FRP reinforcement is either null or extremely small, disturbing the global performance of the considered analytical models. From the above considerations, the consistence of results obtained with the IDB was appraised by means of removing from the analysis those observations, which in the authors' belief, lead into incoherent results. A reduced database (RDB) containing 130 beams extracted from the IDB was assembled. A beam was removed from DB when fulfils one of the following conditions: *i)* statistical outliers; *ii)* beams reinforced with bidirectional fibers; *iii)* reinforcement systems with special anchorage mechanisms; *iv)* beams that show poor performance in all of the aforementioned design models (χ < 0.25).

Figure 5 presents the obtained results with the RDB, providing for each design model a scatterplot of the V_{fd} *vs* $V_{f,exp}$ relationship, an histogram of the χ ratio distribution and a "box and whiskers" plot of the χ ratio variation related with the reinforcement configuration. The box plot diagram graphically depicts the statistical five-number summary, which consists of the smallest non-outlier observation, lower quartile (Q1), median, upper quartile (Q3), and largest non-outlier observation.
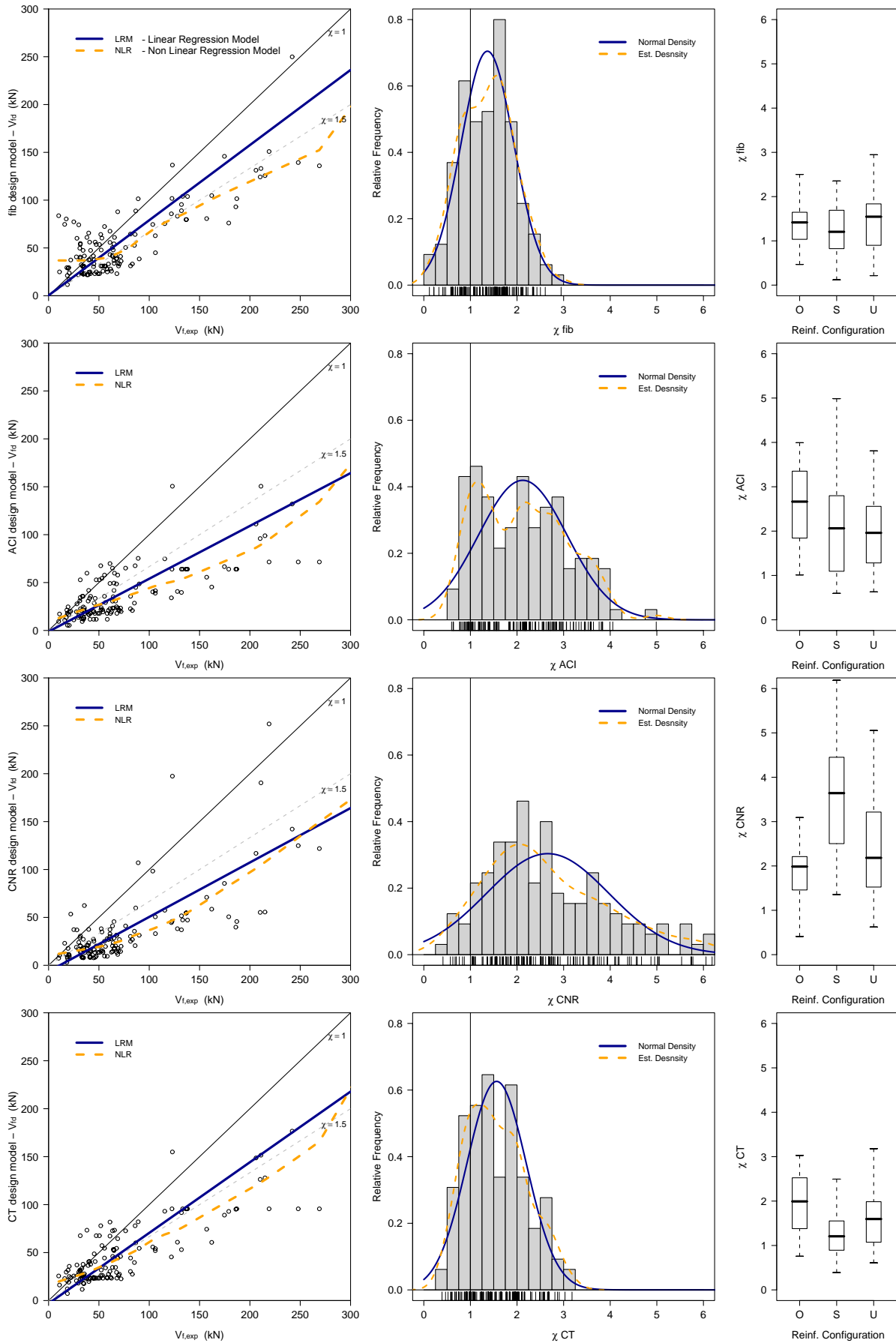
5

Fig. 5 – Analysis results with the RDB (from top to bottom: fib, ACI, CNR and CT design models)

Table 4: Statistical values of the χ factor computed from the RDB

χ	MIN	Q1	MED	AVG	Q3	MAX	STD	COV	$\sum$ PEN
FIB	0.119	0.889	1.389	1.387	1.76	3.278	0.592	0.427	354
ACI	0.596	1.310	2.141	2.221	2.88	5.463	1.066	0.48	233
CNR	0.411	1.734	2.503	2.886	3.69	8.931	1.653	0.573	219
CT	0.39	1.051	1.522	1.655	2.03	5.454	0.784	0.474	294

The values in Table 4 show that, despite the global improvement in the design models performance with the RDB, the results follow the same trend as for the IDB analysis, thus ratifying the consistency of the collected data.

Figure 6 plots the safe (PSS) *vs* unsafe (PAS) predictions diagrams for both the IDB (a) and the RDB (b). From their analysis, it is mandatory to emphasize that all the studied design models show a poor performance taking into account the large amount of unsafe predictions for the design value of the FRP contribution in shear.
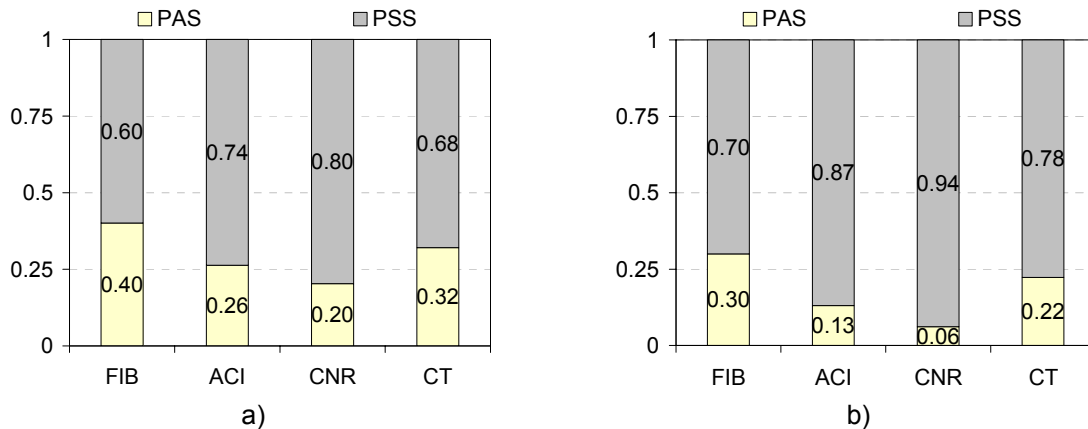

Fig. 6 –PAS and PSS ratios with the: a) IDB, b) RDB

3.4 Influence of other parameters not explicitly considered in the analytical formulations

Such poor performance showed by the aforementioned analytical formulations indicates that the relative influence of the considered parameters is simulated deficiently and the effect of others, not explicitly taken into account, should not be neglected.

Figure 7 presents some relationships that are supposed to affect the performance of the analytical models namely, the shear force gain ratio, $V_{f,exp} / (V_{r,exp} - V_{f,exp})$, the influence of the longitudinal reinforcement percentage, ρ_{sl}, and the influence of shear steel reinforcement presence are investigated.

All the studied analytical formulations seem to show an increase of the χ factor with beams where the global shear force gain is higher. Such trend is observed for both discrete (DISC) and continuous (CONT) reinforcement arrangements, being more obvious for the *fib* and CT models while a more diffuse pattern is observed within the ACI and CNR models.

From the interaction between the χ factor and the longitudinal steel reinforcement it is found that χ tends increase with the increment of the $E_s\rho_s / E_f\rho_f$ ratio suggesting a major interaction between the FRP and longitudinal reinforcement. On the plotted diagrams, beams with conventional shear reinforcement are set aside from those without stirrups decoupling the interactions between these two phenomena. It proved that both kinds of beams (with and without stirrups) follow the same trend regarding the χ *vs* $E_s\rho_s / E_f\rho_f$ relationship.

The plots of the χ *vs* $E_{sw}\rho_{sw} / E_f\rho_f$ relation suggest that beams without stirrups may have higher χ factors with the studied analytical models than those with higher shear reinforcement ratio. Nevertheless it is the authors' belief that the pattern found in the χ *vs* $E_{sw}\rho_{sw} / E_f\rho_f$ scatter when $A_{sw}>0$ may also be influenced by the longitudinal reinforcement ratio. In a future approach these phenomena should be investigated, making several analysis of χ *vs* $E_{sw}\rho_{sw} / E_f\rho_f$ for different clusters of ρ_{sl}.
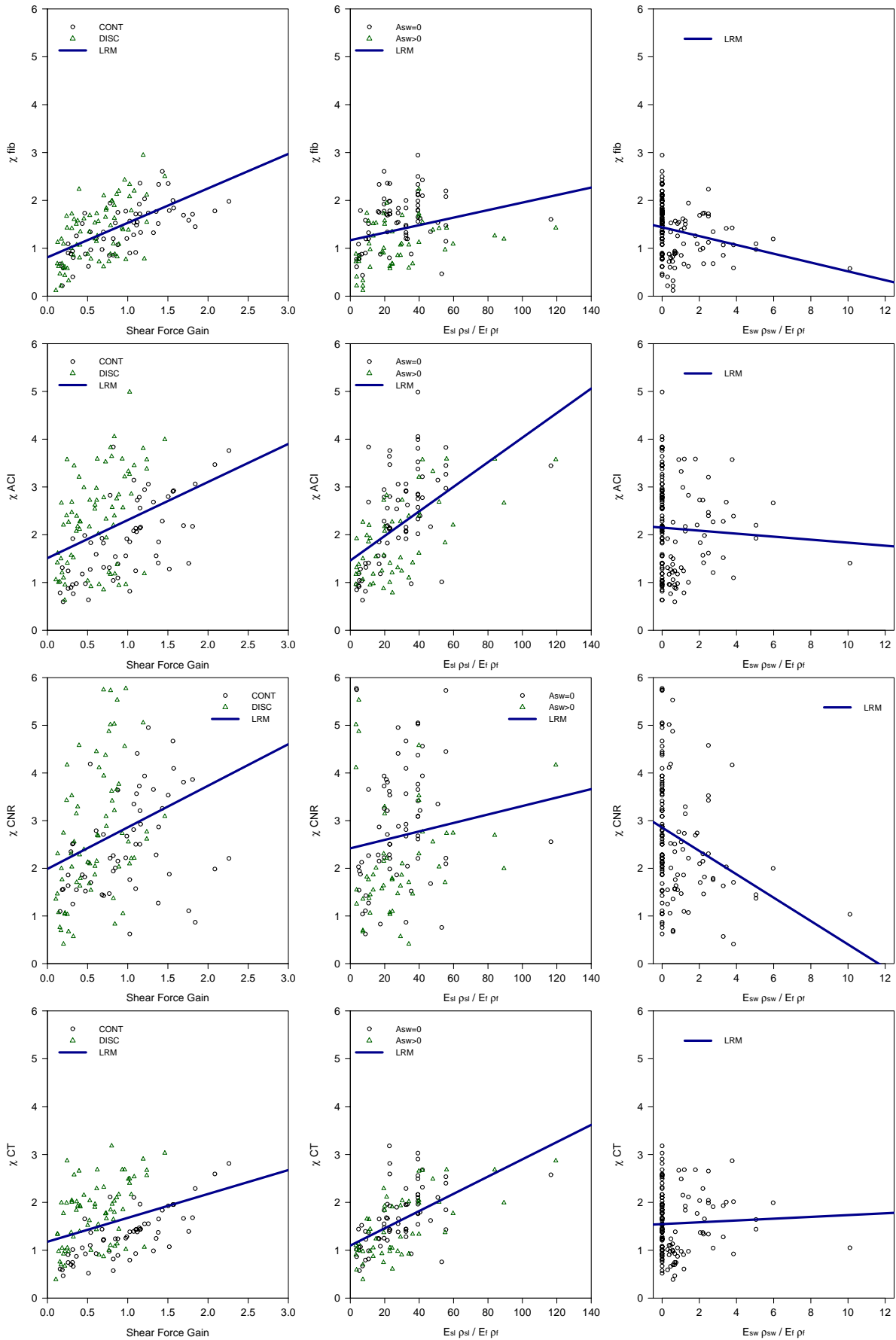
7

Fig. 7 – Influence of shear gain, longitudinal and shear reinforcement on the models performance

4   CONCLUSIONS

Based on the information available in the literature regarding the shear strengthening of RC beams with externally bonded CFRP, a comprehensive database was assembled containing experimental results of 212 beams. The results obtained from a statistical analysis carried out on such database demonstrate that none of the analytical formulations predicts with enough accuracy the contribution of the EBR CFRP systems for the shear strengthening of RC beams. A large scatter of the $\chi=V_{f,exp}/V_{fd}$ was found within all the design models, even when a reduced database (RDB) was used in the analysis.

Using the RDB the average of the χ factor varies between 1.4 (fib) and 2.9 (CNR) and the coefficient of variation is comprehended between 43% (*fib*) and 57% (CNR). From a statistical point of view the CT model can be pointed as the one with the best performance since it always combines an appropriate global safety factor (AVG χ = 1.67) with the one of most least scattered behaviors (COV χ = 47%). Although the large amount of calculated V_{fd} values that are against safety suggest that all of the aforementioned models are still not robust enough for generalized practical design purposes.

A reliability analysis and classification based on structural safety was also implemented. Among the studied formulations, the *fib* design model presented the most unsafe results from all, while the safest results were attained with the CNR design code provisions. CNR also provided the largest amount of extremely conservative predictions especially for the S type strengthening configuration.

The influence of some parameters not explicitly considered on the analytical models was assessed, proving that the performance of the aforementioned design models is subordinated to the global attained shear force gain. Furthermore, the influence of conventional steel reinforcement (longitudinal and transversal) proved to be significant, and none of the studied analytical models explicitly considers these parameters to determine the FRP contribution to shear. Other parameters not taken into account in the analytical formulations may also influence the behavior of strengthened beam. The collected database provides a significant source for data mining techniques in order to decouple the interactions between all the phenomena involved. Thus, more investigation in this field is needed in order to improve the existing design models.

REFERENCES

[1]   Triantafillou, T. "Shear strengthening of reinforced concrete beams using epoxy bonded FRP composites" *ACI Structural Journal* 11, 9 (March-April 1998), 107-115.

[2]   Khalifa *et al* "Contribution of externally bonded FRP to shear capacity of RC flexural member" *Journal of Composites for Construction* ASCE 2, 4 (1998), 195-202.

[3]   Monti, G., and Liotta, M. "FRP-strengthening in shear: tests and design equations". em *7th International Symposium on Fiber Reinforced Polymer (FRP) Reinforcement for Concrete Structures (FRP7RCS)*, 2005, ACI Symposium Publication 230.

[4]   fib "*Bulletin 14 - Externally Bonded FRP reinforcement for RC structures*" Technical report, 2001, Task Group 9.3 FRP (fibre reinforced polymer) reinforcement for concrete structures.

[5]   ACI "*440.2R-02: Guide for the design and construction of externally bonded FRP systems for strengthening of concrete structures*", 2002, Reported by ACI Committee 440.

[6]   CNR-DT200 "*Guidelines for design, execution and control of strengthening interventions by means of fibre reinforced composites*", 2004, National Research Council.

[7]   CIDAR - "*Design guideline for RC structures retrofitted with FRP and metal plates: beams and slabs*" Draft 3 - submitted to Standards Australia, 2006, The University of Adelaide.

[8]   Chen, J.F. e Teng, J.G. - "Shear Capacity of FRP Strengthened RC Beams: FRP Rupture" *Journal of Structural Engineering*, ASCE 2003: 129(5): 615–625.

[9]   Chen, J.F. e Teng, J.G. - "Shear Capacity of FRP Strengthened RC Beams: FRP Debonding" *Construction and Building Materials* 2003: 17(1): 27– 41.

[10]   ACI 318 "*318-02/318R-02: Building code requirements for structural concrete and commentary*", 2002, Reported by ACI Committee 318.

[11]   Bousselham, A., and Chaallal, O. "Shear strengthening reinforced concrete beams with fiber reinforced polymer: assessment of influencing parameters and required research". *ACI Structural Journal* 110, 2 (March-April 2004), 219-227.

[12]   Aprile, A., and Benedetti, A. "Coupled flexural-shear design of R/C beams strengthened with FRP" *Composites Part B: Engineering* 35, 1 (January 2004), 1-25.

[13]   Lima, J.L.T. "*Assessment of the effective strain in FRP laminates used in shear strengthening of reinforced concrete beams*", MSc thesis (in preparation) 2006, Univ. Minho, Portugal.

[14]   Collins, M.P. - "*Evaluation of shear design procedures for concrete structures*", 2001, A Report prepared for the CSA technical committee on reinforced concrete design.